

Fin Gaps and Body Slots: Effects and Modeling for Projectiles and Missiles

Ameer G. Mikhail*

U.S. Army Ballistic Research Laboratory, Aberdeen Proving Ground, Maryland

All known prior work concerned with the effect of streamwise fin-body gaps (unporting effect) and body slots on the fin loads of missiles and projectiles in the transonic speed regime of $0.8 \leq M \leq 1.2$ has been surveyed and analyzed. All known experimental data for the gap effects have been analyzed. A correlation relation was established to predict fin normal force losses due to gaps for any fin shape, size, aspect ratio, gap/body-diameter ratio, body diameter, and flow Reynolds number. The results match well with the data, which span a large variation in Reynolds numbers, body diameter, and boundary-layer thickness. Although the Mach range for the present model was intended to be $0.8 \leq M \leq 1.2$, available data indicated its validity in the wider range of $0.7 \leq M \leq 1.8$. Fifteen cases were utilized to validate the present gap model. The slot effect model used is that of Washington et al. Application of these two corrections to the Copperhead guided projectile was made, and a reduction as large as 38% was predicted for the normal force, which was then validated by the experimental data. The present results can be used for estimating fin-load losses for the fin design of guided projectiles and missiles, with an accuracy of $\pm 5\%$ over the intended Mach number range $0.8 \leq M \leq 1.2$ and for a gap/diameter ratio ≤ 0.08 .

Nomenclature

A, A_1, A_2	= fin total surface area (one side only)
$A_{10}, A_{11}, A_{20}, A_{22}$	= fin partial surface area (one side only)
R	= fin aspect ratio, $(2b)^2/S$
A_f	= fin surface area (one side only of one fin panel)
A_g	= streamwise gap area for one fin panel
AF	= fin area correlation factor
b	= fin semispan (without a gap)
b_1, b_2	= a prescribed fin height (without a gap)
BF	= boundary-layer correlation factor
c, c_1, c_2	= fin-root chord length
CF	= overall fin correlation factor
C_N	= normal force coefficient (based on the body reference area) = normal force/ qS_{ref}
C_{Nf}	= fin (and its interference) normal force coefficient based on the body reference area
C_{Nfg}	= fin (and its interference) normal force coefficient, in presence of a fin gap g
$C_{N\alpha}$	= normal-force-slope coefficient, per rad, $\partial C_N / \partial \alpha$
$C_{N\alpha f}$	= fin (and its interference) normal-force-slope coefficient, per rad
$C_{N\alpha fg}$	= fin (and its interference) normal-force-slope coefficient, in presence of a fin gap g , per rad
C_M	= pitching moment coefficient about the c.g. of the configuration, (pitching moment)/ $qS_{ref}D$
$C_{M\alpha}$	= pitching moment slope coefficient, per rad, $\partial C_M / \partial \alpha$
$C_{M\alpha g}$	= pitching moment slope coefficient, per rad, in the presence of a fin gap g
CSF	= fin chord and span correlation factor
D	= body diameter

FNF	= fin normal force loss factor, resulting from presence of a fin gap g
g, g_1, g_2	= gap height between fin-root chord and body surface
GF	= fin gap correlation factor
M	= Mach number of projectile
q	= dynamic pressure of the flow $(0.5 \rho_\infty U_\infty^2)$
Re, Re_1, Re_2	= Reynolds number per unit length, $\rho_\infty U_\infty / \mu_\infty$
Re_x	= local Reynolds number of the projectile flow, $\rho_\infty U_\infty X / \mu_\infty$
S	= fin surface area (one side) of two fin panels connected without gaps
S_{ref}	= body reference area, $\pi D^2/4$
SF	= fin shape correlation factor
U	= projectile velocity
x	= distance, along the body axis, from the nose tip
x_{LE}, x_{LE1}, x_{LE2}	= distance, along the body axis, from the nose tip to the leading edge of a fin panel, at the fin-root section
α	= angle of attack
α_t	= total angle of attack $\approx \sqrt{\alpha^2 + \beta^2}$ (for small α and β)
β	= sideslip angle
δ	= boundary-layer thickness
$\delta_{LE}, \delta_{LE1}, \delta_{LE2}$	= boundary-layer thickness at the leading edge of the fin-root section
ρ	= air density
μ	= molecular viscosity coefficient
Subscripts	
g	= indicates the presence of a gap between fin-root chord and body surface
s	= indicates the presence of open slot(s) on the projectile body near the fin panel
∞	= indicates undisturbed freestream condition

Presented as Paper 87-0447 at the AIAA 25th Aerospace Sciences Meeting, Reno, NV, Jan. 12-15, 1987; received Jan. 30, 1987; revision received Nov. 23, 1987. This paper is declared a work of the U.S. Government and is not subject to copyright protection in the United States.

*Aerospace Engineer, Launch and Flight Division. Member AIAA.

I. Introduction

As reported in Ref. 1, large deviations were noticed between both the pitching moment and normal force predictions and wind-tunnel data for the aerodynamic prediction of the

Copperhead guided projectile shown in Fig. 1. Two predictions were made using the fast aerodynamic design codes of the Missile DATCOM and the NSWCAP, both of which are described in Ref. 1. This deviation was as large as 38% at $M \approx 1$ and was generally quite large in the speed regime of $0.8 < M < 1.2$. This deviation was significantly smaller outside that speed regime, i.e., in the regimes $0.5 \leq M < 0.8$ and $1.2 < M \leq 1.8$. This large deviation was attributed mainly to the effects of the tail-fin gaps and the open slots in the projectile body. These slots are used to house the fin blades before in-flight deployment. The tail-fin geometry and the associated streamwise gaps can be found in Ref. 2.

It is the purpose of this paper to compute the normal-force losses of the fins owing to streamwise fin-body gaps and body slots, in the transonic regime $0.8 \leq M \leq 1.2$ for $g/D \leq 0.08$. All known data concerned with these effects have been utilized for establishing the present correlations.

Gap Effects

Bleviss and Struble³ in 1953 apparently were first to present an inviscid analysis of gap losses for triangular fins at supersonic speeds, $M \geq 1$. The analysis is valid only for triangular fins and is not applicable for small gap/diameter ratios, where viscosity effects are dominant. The analysis also assumes a long afterbody extending beyond the fin location. Streamwise gap refers to the gap when the control surface is aligned along the axial direction of the body. At almost the same time, Mirles⁴ presented a slender-body analytic solution for the fin-lift losses for the same triangular fins and long afterbody limitations. Therefore, his results were expectedly close to those of Ref. 3. Shortly thereafter, in 1954, Dugan and Hikido⁵ also presented slender-body analysis for gap effects for triangular fins mounted on long afterbodies. The results, being based on slender-body theory, are Mach number independent and not restricted to supersonic speeds. Hoerner,⁶ in a book published in 1975, refers to some very early experiments (probably in the 1930's) at very low subsonic speeds for low-aspect-ratio fins. The presented data are very sparse, and the test conditions are very ambiguous.

In 1964, the first wind-tunnel tests for gap effects were presented by Killough.⁷ Data were provided for three rectangular fins of aspect ratio 1.0, 2.0, and 3.0 in the Mach range 0.8–4.5. A similar wind-tunnel data set was obtained later by Dahlke and Pettis⁸ in 1970 for a single triangular fin of $AR = 1.5$ and three rectangular fins of $AR = 0.5, 0.75$, and 1.0. These fins were tested in the Mach range 0.8–4.0 for four gap heights. In 1977, although studying other effects, Henderson⁹ tested a rectangular fin of $AR = 1.67$ for a single gap height in the Mach range $0.8 \leq M \leq 1.2$. In 1982, Fellows¹⁰ provided subsonic data for two sets of rectangular fins of $AR = 1.67$ and 2.22 for very small gap heights.

In 1982, August¹¹ used the inviscid supersonic analysis of Bleviss and Struble³ and the manipulated results of Hoerner at subsonic speeds to estimate the normal-force losses for stream-

wise gaps. Application was made to a triangular fin of aspect ratio 1.0. August applied the analysis to the Sidewinder missile geometry at $M = 2.5$ for the triangular canard fin with fin deflection. The gap area was estimated and equalized by a streamwise gap area. This application was done during the development of a fast aerodynamic design code. Sun et al.,¹² in 1984, reiterated the results of August and made an application to a missile configuration at $M = 1.2$ and 2.0 using the same computer code.

Slot Effects

Less exhaustive data and analyses have been pursued by investigators for the slot effects than those pursued for the gap effects. In 1979, Appich and Wittmeyer¹³ tested a full-scale model of the Copperhead projectile and reported the effect of closing the slots on the normal force and drag of the projectile in the Mach range 0.5–1.8. However, results were presented only for $M = 0.5$ and 1.5. Washington et al.¹⁴ analyzed the data of Appich and Wittmeyer¹³ and suggested a simple model to correct for the normal-force losses due to the slots. This correction utilizes slender-body theory and is, therefore, independent of Mach number. However, applications were made only to subsonic speeds of $M = 0.5, 0.8$, and 0.95. The same results were summarized later in Ref. 15. The axial force and drag contribution of the slots were studied and reported separately by Appich et al. in 1980.¹⁶

II. Analysis

Gap Effects

An analytic correlation for the fin-body gap effects is established in this section, taking into account all existing data for fin gaps. This correlation is intended for the transonic Mach range of $0.8 \leq M \leq 1.2$ and for $g/D \leq 0.08$. However, existing data show its applicability in the wider range of $0.7 < M < 1.8$ without loss in accuracy.

Details of the Experimental Data and Test Conditions Used

The four wind-tunnel data sets of Refs. 7–10 were used. The exact body configuration, fin shape, and dimensions for each test are given in Ref. 2. The test conditions, including Mach and Reynolds numbers, gap height, and gap fin area ratio, for each case are given in Table 1.

Correlation Relation

Based on the familiar work of Pettis et al.,¹⁷ the normal-force coefficient of a combined missile body and fins is usually written as

$$C_{N_{BT}} = C_{N_B} + (K_{T(B)} + K_{B(T)})C_{N_T} \quad (1)$$

where the subscripts B , T , and BT stand for body alone, tail alone, and body-tail combination, respectively; $K_{T(B)}$ is the interference factor representing the increase of tail-fin lift due to

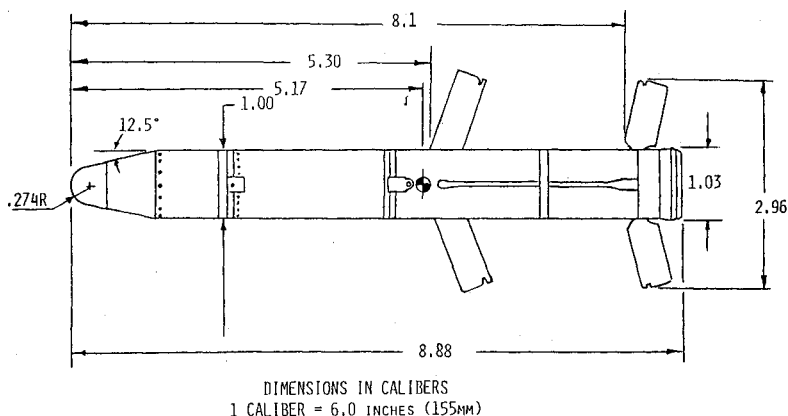


Fig. 1 Configuration of the Copperhead projectile.

the existence of a nearby body and is usually referred to as the body upwash effect; and $K_{B(T)}$ is the interference factor representing the increase of body lift due to the existence of a nearby tail fin and is usually referred to as the carryover factor. This interference is represented as a small fraction of the fin-alone lift.

In the present work C_{N_f} denotes the fin normal-force plus the two mentioned interference effects, i.e., Eq. (1) can be written as

$$C_{N_{BT}} = C_{N_B} + C_{N_f} \quad (2)$$

For a gap of any size, the lift (and therefore the normal force) produced by a fin would always be less than that without a gap. Therefore, a normal-force loss factor, FNF, is introduced and is defined as

$$\text{FNF} = \frac{C_{N_{fg}}}{C_{N_f}} = \frac{C_{N_{fg}}}{C_{N_{af}}} \quad (3)$$

where $C_{N_{fg}}$ is the normal force of the fin (including the interference effects) in the presence of a gap. The second equality sign in Eq. (3) is valid only for small angles of attack, usually less than ± 6 deg. For a case with gap, one could easily model the effect of a gap if the loss factor FNF were known. This modeling is achieved through the equation

$$C_{N_{BT}} = C_{N_B} + \text{FNF} \cdot (K_{T(B)} + K_{B(T)})C_{N_T} \quad (4)$$

One approach considered for modeling was to correct the analysis of Bleviss and Struble³ of triangular fins to account for viscosity and shape of fin planform. The baseline case would be the triangular fin data of Dahlke and Pettis.⁸ However, this complex formulation was not chosen in favor of a different and simpler approach. The new approach is to make all corrections and/or correlations based on the same triangular fin shape for which an inviscid analysis could be valid and to base all the correlation relations on experimental data. Therefore, the FNF factor was computed for all of the test cases of Refs. 7-10, and their wind-tunnel test conditions were determined. The intent

was to correlate a known FNF for a known fin planform of certain gap height, mounted on a particular body diameter in a flow of particular Reynolds number, to the FNF of a totally different fin with all different parameters. Figure 2 shows fin configurations 1 and 2 where subscript 1 will always refer to the known case and 2 to the unknown case. The planform of fin 2 is split into two parts: a basic triangular configuration of area A_{22} and a second part, which is the remainder of the planform area with an area designated as A_{20} . Examples of the area A_{22} designation for several fin planforms are given in Fig. 3.

The FNF factor is thought to be a function of several parameters: FNF = FNF (fin area, fin shape, fin-gap height, gap/diameter ratio, Reynolds number at the leading edge of fin, fin aspect ratio, Mach number).

The last two parameters were later deleted for the following reasons: The aspect ratio was substituted by both the fin area and fin shape parameters. The fin shape is represented not only by a description factor (e.g., triangular or rectangular) but also by the root chord and the semispan height. The Mach number dependency in the FNF function was dropped when the data of Dahlke et al. were analyzed in the transonic region of $0.8 \leq M \leq 1.2$. These data, examples of which are given in Fig. 4, showed little variation in the FNF with Mach number. This behavior was noticed in all data. Thus, although both C_{N_f} and $C_{N_{fg}}$ do change, their ratio is always constant in that transonic speed range. Furthermore, by computing the FNF factor for another fin planform of Dahlke et al.⁸ one can notice that the Mach number independence extends between $M = 0.7$ and 1.8. This observation is depicted in Fig. 5. One also can notice the surprising change in FNF in the subsonic region $M < 0.7$. For that reason, i.e., the rapid change of FNF in the subsonic region, the results of Hoerner should be used with caution.

The basic correlation formula relates the unknown case 2 to the known case 1 through the overall correlation factor CF as

$$\left. \frac{C_{N_{fg}}}{C_{N_{af}}} \right|_2 = \text{CF} \cdot \left. \frac{C_{N_{fg}}}{C_{N_{af}}} \right|_1 \quad (5)$$

i.e.,

$$\text{FNF}_2 = \text{CF} \cdot \text{FNF}_1$$

This overall correlation factor itself is split into a multiple of several factors. They are: the fin shape factor SF; fin area factor AF; fin-gap factor GF; fin chord/span factor CSF; and boundary-layer factor BF. Therefore, one can write:

$$\begin{aligned} \left. \frac{C_{N_{fg}}}{C_{N_{af}}} \right|_2 &\equiv \text{FNF}_2 = \text{CF} \cdot \text{FNF}_1 \\ &= [\text{SF} \cdot \text{AF} \cdot \text{GF} \cdot \text{CSF} \cdot \text{BF}] \left. \frac{C_{N_{fg}}}{C_{N_{af}}} \right|_1 \end{aligned} \quad (6)$$

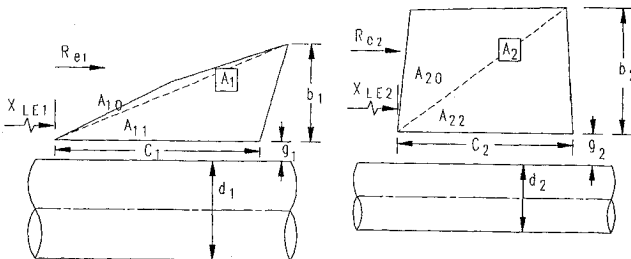


Fig. 2 Nomenclature for the correlation analysis.

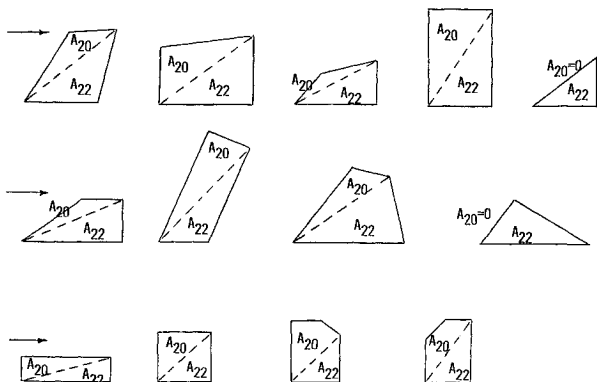


Fig. 3 Examples of fin area designation for several fin planforms.

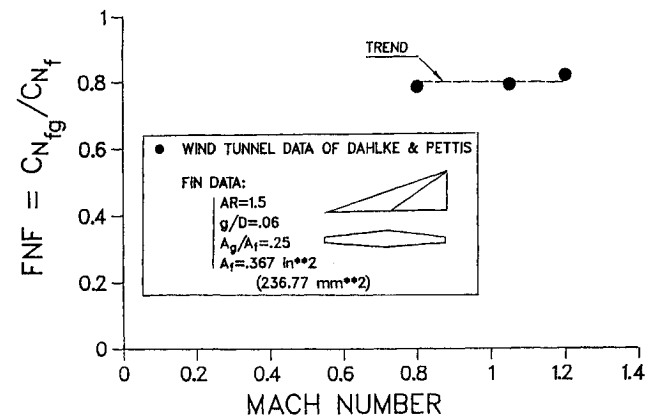
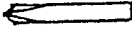

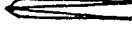




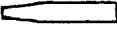
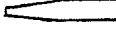

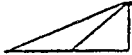





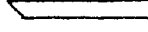
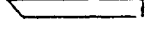




Fig. 4 Transonic wind-tunnel data for triangular fin of $AR = 1.5$.

Table 1 Test conditions for all data utilized

Killough's data (1964)				
				
				
$D = 1.0$ in. (25.4)	$R = 1.0$	$R = 2.0$	$R = 3.0$	
$M = 0.8$ to 4.5	$Af = 0.3663$	$Af = 0.3364$	$Af = 0.3358$	
$Re = 0.4 \times 10^6$ /in.	$g/D - (Ag/Af)$	$g/D - (Ag/Af)$	$g/D - (Ag/Af)$	
(0.157×10^6 /cm)	0.0-(0.0)	0.0-(0.0)	0.0-(0.0)	
	0.08-(0.187)	0.08-(0.138)	0.08-(0.113)	
	0.16-(0.374)	0.16-(0.276)		
	0.25-(0.584)	0.25-(0.430)		
Dahlke and Pettis' data (1970)				
				
				
$R = 1.5$	$R = 0.5$	$R = 0.75$	$R = 1.0$	$D = 1.1$ in. (27.94 mm)
$Af = 0.3675$	$Af = 0.490$	$Af = 0.7350$	$Af = 0.4437$	$M = 0.8$ to 4.5
$g/D - (Ag/Af)$	$g/D - (Ag/Af)$	$g/D - (Ag/Af)$	$g/D - (Ag/Af)$	$Re = 0.415 \times 10^6$ /in.
0.00-(0.0)	0.00-(0.0)	0.00-(0.0)	0.00-(0.0)	(0.163×10^6 /cm)
0.06-(0.251)	0.06-(0.188)	0.06-(0.126)	0.08-(0.187)	
0.12-(0.502)	0.12-(0.377)	0.12-(0.251)	0.16-(0.374)	
0.20-(0.837)	0.20-(0.638)	0.20-(0.419)	0.25-(0.584)	
Henderson's data (1977)				
				
				
$D = 5.0$ in. (127.0 mm)			$R = 1.67$	
$M = 0.7$ to 1.2			$Af = 7.500$	
$Re = 0.316 \times 10^6$ /in.			$g/D - (Ag/Af)$	
(0.124 $\times 10^6$ /cm)			0.0-(0.0)	
			0.5-(0.10)	
Fellows' data (1982)				
$D = 5.905$ in. (150.0 mm)				
$M = 0.6$ and 0.85				
$Re = 0.287 \times 10^6$ /in. ($M = 0.6$)			$R = 1.67$	$R = 2.22$
(0.113 $\times 10^6$ /cm)			$Af = 3.767$	$Af = 5.022$
0.340×10^6 /in. ($M = 0.85$)			$g/D - (Ag/Af)$	$g/D - (Ag/Af)$
(0.134 $\times 10^6$ /cm)			0.0-(0.0)	0.0-(0.0)
			0.02-(0.66)	0.02-(0.05)
Dimensions in inches; area in inches ²				
1 in. = 25.4 mm; 1 in. ² = 645.16 mm ²				

1) The shape factor SF was originally formulated as

$$SF = (A_2/A_{22})/(A_1/A_{11}) = [(A_{22} + A_{20})/A_{22}]/[(A_{11} + A_{10})/A_{11}] \quad (7)$$

This gives a value of 2 for a general correlation from a triangular to a rectangular fin shape and 1 for a general correlation from a rectangular to a rectangular fin.

From the data of Dahlke et al., however, it was found that SF should be 1.76 for a triangular to rectangular shape correlation with $A_{22} = A_{11}$ and with all other conditions fixed. This was finally achieved by recasting Eq. (7) into a slightly more complex form

$$SF = \frac{[(0.76A_{20} + A_{22})/A_{22}] + [0.24A_{20}(A_{22} - A_{11})/0.5b_2c_2(0.5b_2c_2 - 0.5b_1c_1)]}{[(0.76A_{10} + A_{11})/A_{11}] + [0.24A_{10}(A_{22} - A_{11})/0.5b_1c_1(0.5b_2c_2 - 0.5b_1c_1)]} \quad (8a)$$

One can easily track the origin for the split-up factors of 0.76 and 0.24. Also, one can note that the second term in each bracket will drop out if $A_{22} = A_{11}$, for which case the bracket $(0.5b_2c_2 - 0.5b_1c_1)$ in the denominator will also be zero.

2) The surface area correlation factor AF is simply the ratio of the fin total areas (one side only)

$$AF = A_1/A_2 \quad (8b)$$

The reverse order of A_2 to A_1 is logical since if $A_2 > A_1$, one would expect the lift losses to be smaller. This would be due to the contribution of lift produced by A_{20} , which should be affected very little by the gap that dominates the lower area of A_{22} .

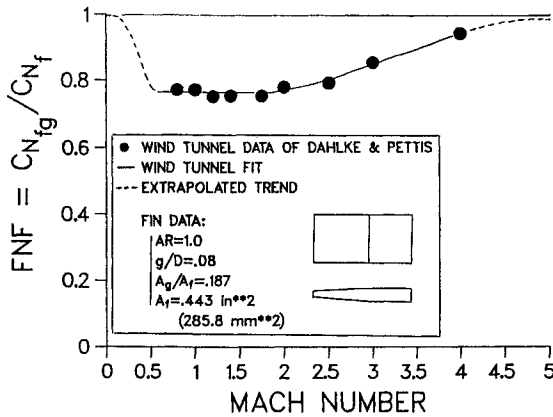


Fig. 5 Wind-tunnel data for rectangular fin of $AR = 1.0$.

3) The gap-height correlation factor GF was found to be

$$GF = \left[\frac{(g/D)_1}{(g/D)_2} \right]^{1/\left[1.6 - \frac{(g/D)_1}{(g/D)_2} \cdot \left(\frac{(g/D)_2 - 0.04}{0.05} \right) \right]} \quad (8c)$$

where, if $(g/D)_2 = 0.04$, GF will be simply

$$GF = [(g/D)_1/(g/D)_2]^{1/1.6}$$

One should note that the correlation employs the gap/diameter ratio rather than the absolute gap height only.

4) The chord/span factor CSF was found to be in the form

$$CSF = \sqrt{(b_2/b_1)(c_2/c_1)} \quad (8d)$$

where b_2 and b_1 are not, in general, equal to the semispan height but rather the top apex height for the triangular areas A_{22} and A_{11} , respectively. This can be shown if Fig. 2 is considered and the concept is applied to the many planforms of Fig. 3. For many fin planforms, however, b_2 and b_1 can be the same as the fin semispans.

5) The boundary-layer factor BF was based on the boundary-layer thickness at the leading edge of the fin at the fin-root section. It was found appropriate to write

$$BF = (\delta_{LE2}/\delta_{LE1})^{0.88} \quad (8e)$$

where the boundary-layer thickness δ_{LE} was estimated by the familiar form¹⁸ for turbulent boundary layers in axisymmetric tubes,

$$\delta_{LE1} = 0.37X_{LE1}/(R_{eX_{LE1}})^{0.2}$$

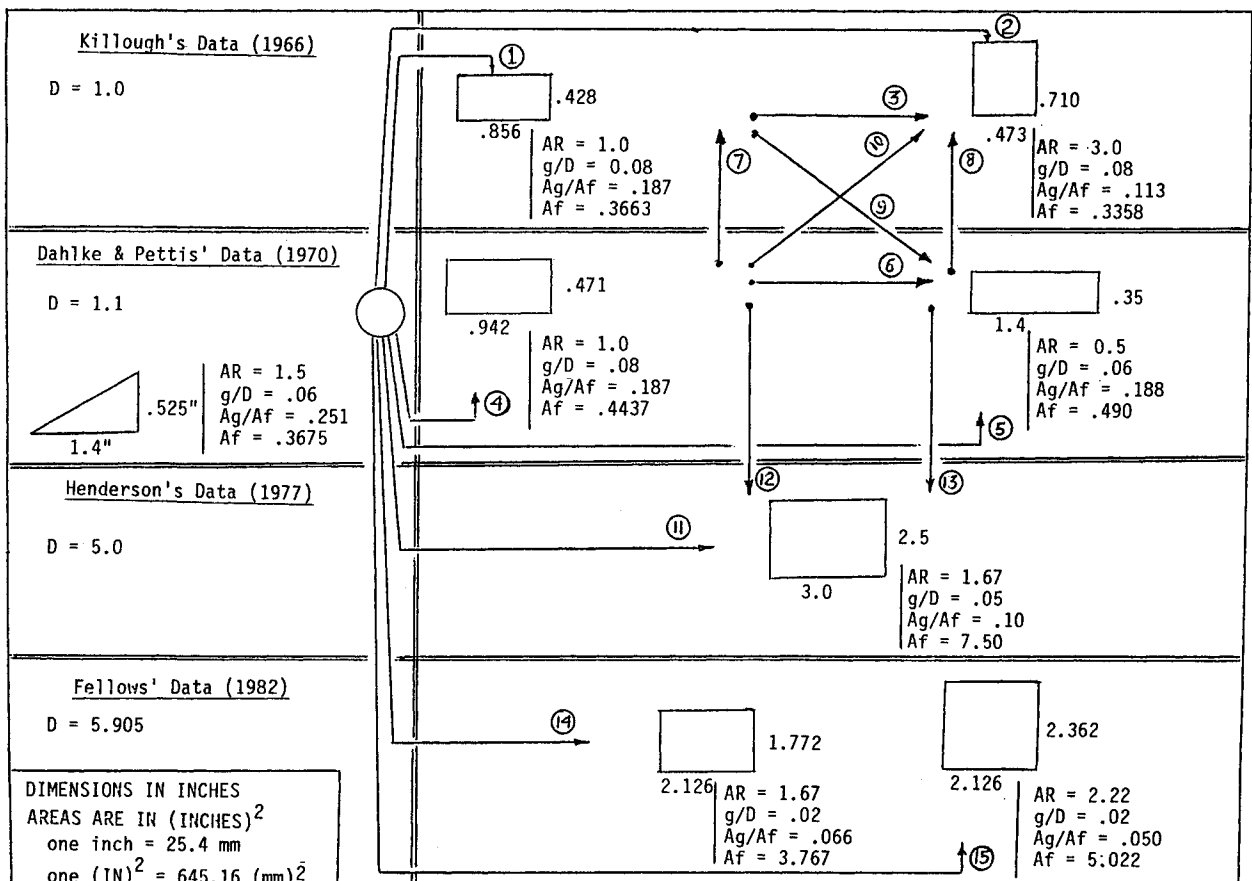
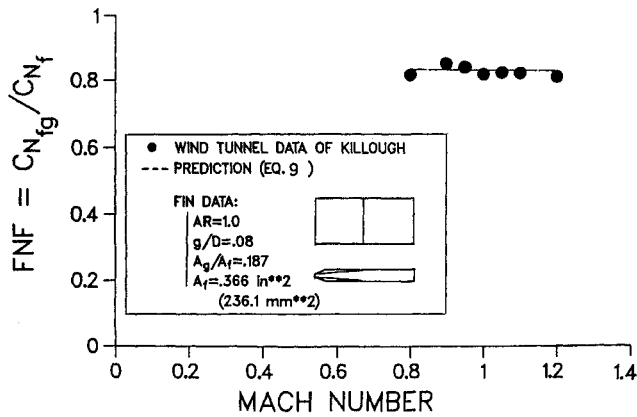
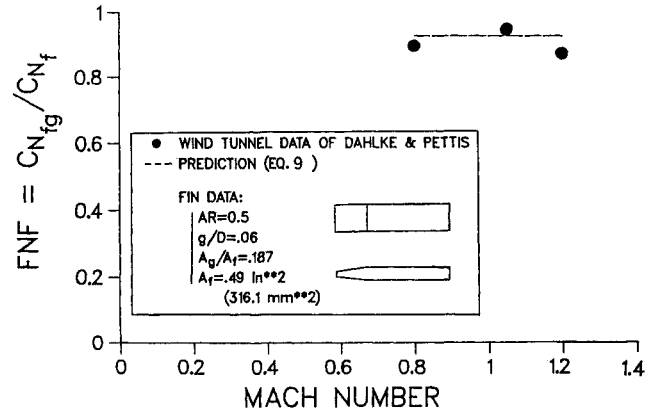
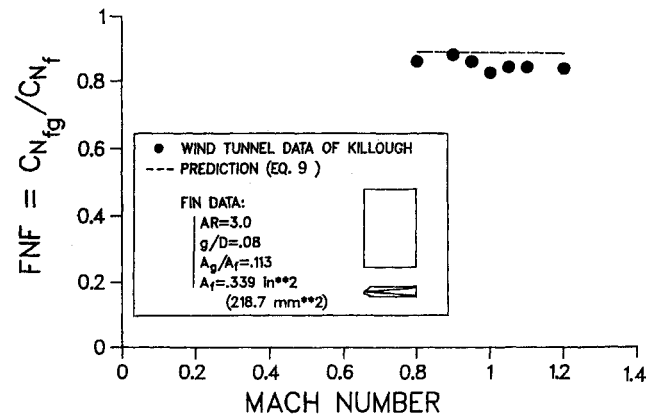
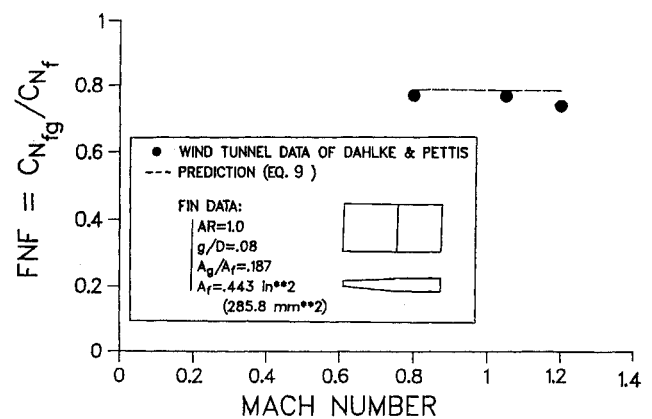


Fig. 6 Case designation for the 15 correlation tests used for validation.

Fig. 7a Comparison with data of Killough, rectangular fin of $AR = 1.0$.Fig. 8a Comparison with data of Dahlke and Pettis, rectangular fin of $AR = 1.0$.Fig. 7b Comparison with data of Killough, rectangular fin of $AR = 3.0$.Fig. 8b Comparison with data of Dahlke and Pettis, rectangular fin of $AR = 0.5$.

Finally, one summarizes the fin normal force loss correlation factor as

$$FNF_2 \equiv \frac{C_{N_{sf2}}}{C_{N_{sf1}}} = \left[\left\{ \frac{(0.76A_{20} + A_{22})}{A_{22}} + \frac{0.24A_{20}(A_{22} - A_{11})}{(0.5b_2c_2)(0.5b_2c_2 - 0.5b_1c_1)} \right\} \right. \\ \left. \left\{ \frac{(0.76A_{10} + A_{11})}{A_{11}} + \frac{0.24A_{10}(A_{22} - A_{11})}{(0.5b_1c_1)(0.5b_2c_2 - 0.5b_1c_1)} \right\} \right] \\ \times \frac{A_1}{A_2} \times \left\{ \left(\frac{(g/D)_1}{(g/D)_2} \right)^{1.6} \left[\frac{(g/D)_1}{(g/D)_2} - \frac{0.04}{0.05} \right] \right\} \times \left\{ \sqrt{\left(\frac{b_2}{b_1} \right) \left(\frac{c_2}{c_1} \right)} \right\} \times \left\{ \left(\frac{\delta_{LE2}}{\delta_{LE1}} \right)^{0.88} \right\} \times \frac{C_{N_{sf2}}}{C_{N_{sf1}}} \quad (9)$$

which can be used to predict the losses for a new fin, 2, based on the known losses of another totally different fin, 1, under different flow conditions.

For the direct prediction of losses for any fin, it was decided that the triangular fin of Dahlke and Pettis would be used at $g/D = 0.06$, as the known reference case. This choice was made in order that future corrections to the analysis of Bleviss and Struble would be applicable to that configuration. Knowing the geometric data of that reference fin and its normal fin-loss factor, predicting $(C_{N_{sf2}}/C_{N_{sf1}})_2$ for any fin should be made using Eq. (9). The data for that reference triangular fin is: $A_{10} = 0$, $A_{11} = 0.3675 \text{ in.}^2$ (237.09 mm²), $A_1 = 0.3675 \text{ in.}^2$ (237.09 mm²), $b_1 = 0.525 \text{ in.}$ (13.33 mm), $c_1 = 1.4 \text{ in.}$ (35.56 mm), $(g/D)_1 = 0.06$, $\delta_{LE1} = 0.1934 \text{ in.}$ (4.912 mm), and $FNF_1 = 0.795$.

Slot Effects

Only effects on the fin normal force are considered. The effects on axial forces are discussed in Ref. 16, but they are not

considered in this work. The approach used here is that of Washington et al.,^{14,15} which is briefly summarized. The carry-over lift factor $K_{B(T)}$ of Eq. (1), which represents the increase in body lift due to the presence of the fin, is eliminated. That is to say, with the existence of a slot at or near the fin-root chord, the contribution of the fin to the body lift is negligible. Washington et al.,¹⁴ showed that this approach yielded the observed normal force loss measured in the wind tunnel. The results obtained were good for small α ($< \pm 6$ deg) and for subsonic speeds only ($M = 0.5-0.95$). Because the analysis was based on slender-body theory (independent of Mach number), that approach was applied here up to Mach number 1.2. Based on physical considerations, one should expect a smaller effect of slots at higher supersonic speeds. Therefore, that approach might not be applicable in high supersonic speeds. Another point to be made is that this approach does not account for the slot location, shape, area, or depth. It would be helpful if experimental data were available for those specific areas of interest.

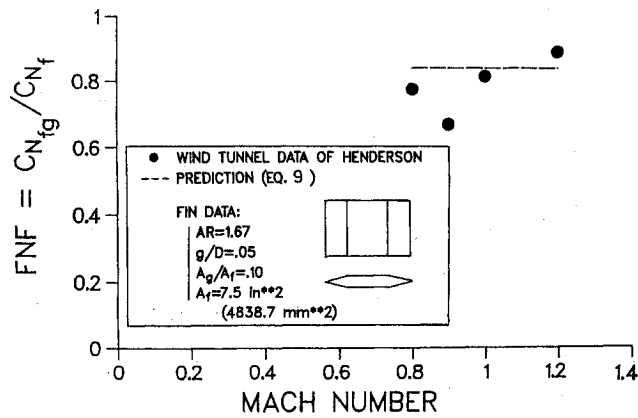


Fig. 9 Comparison with data of Henderson, rectangular fin of $AR = 1.67$.

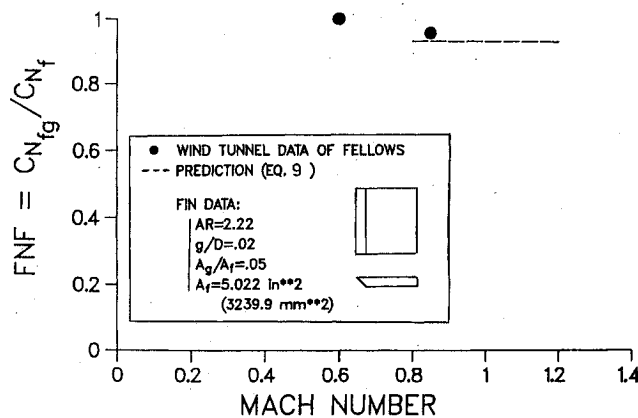


Fig. 10 Comparison with data of Fellows, rectangular fin of $AR = 2.22$.

III. Results

Gap Effects

Validation of the Gap Model

Fifteen cases for validation of Eq. (9) were made using the four data sets for gaps.⁷⁻¹⁰ Cross-correlations were made for every shape, aspect ratio, gap height, body diameter, and Reynolds number. All of the case designation numbers are given in Fig. 6. The baseline case, as referred to earlier, is the triangular fin shape of Dahlke et al. with $g/D = 0.06$. The results using that correlation, with reference to Killough's two cases of $AR = 1.0$ and 3.0 , are given in Figs. 7a and 7b. The prediction is shown to be very good. The results of the application of Eq. (9) to other two-fin cases of Dahlke et al. of $AR = 0.5$ and 1.0 , are shown in Figs. 8a and 8b where the agreement is excellent. The results of applying Eq. (9) to the single-fin shape of Henderson is given in Fig. 9, and the predicted value is shown. It should be mentioned that the single case of Henderson showed large disagreement with those of Dahlke et al., which are more uniform and more trustworthy, as indicated in Henderson's report.⁹ Application of Eq. (9) to the case of Fellows at $M = 0.8$ for a fin of $AR = 2.22$ also resulted in good agreement, as shown in Fig. 10. The data point at $M = 0.6$ is outside the intended Mach region, and it shows a value close to 0.977 . However, this single data point could not be used to establish a model for the subsonic regime of $M < 0.7$. The trend of this result at $M = 0.6$ agrees with the trend postulated and shown in Fig. 5, where a sudden rise in the value of FNF is expected toward $M = 0$. The remainder of the 15 cases are given in Table 2, along with comparisons with the deduced wind-tunnel results.

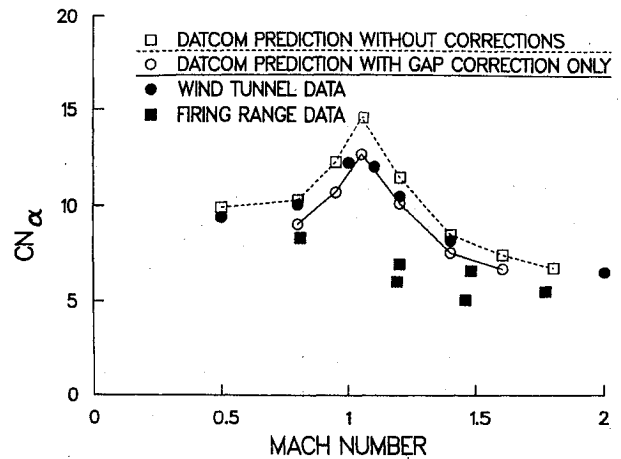


Fig. 11 Gap modeling effect on the normal-force-slope coefficient for the Copperhead projectile.

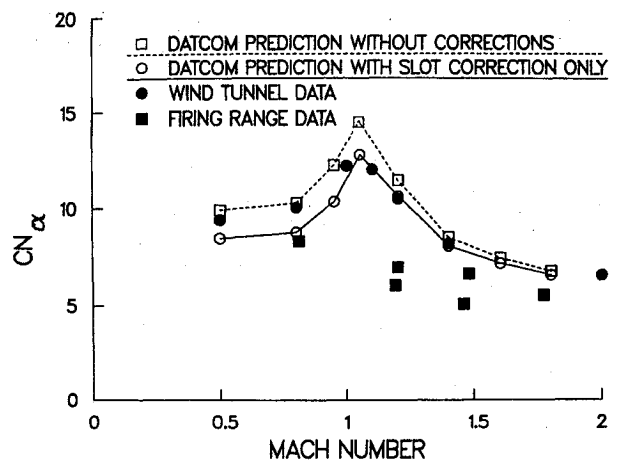


Fig. 12 Slot modeling effect on the normal-force-slope coefficient for the Copperhead projectile.

Table 2 Results of the present analysis for 15 test cases

Correlation case no.	Correlation factor (CF)		Fin normal force reduction factor (FNF)	
	Prediction, Eq. (8)	Wind tunnel	Prediction, Eq. (9)	Wind tunnel
1	1.045	1.04	0.831	0.826
2	1.114	1.07	0.886	0.851
3	1.069	1.03	0.883	0.851
4	0.99	0.956	0.787	0.760
5	1.225 ^a	1.132 ^a	0.974 ^a	0.90 ^a
6	1.213 ^a	1.184 ^a	0.922 ^a	0.90 ^a
7	1.05	1.09	0.800	0.826
8	0.91 ^a	0.945 ^a	0.819 ^a	0.851 ^a
9	1.153 ^a	1.09 ^a	0.952 ^a	0.90 ^a
10	1.093	1.12	0.831	0.851
11	1.053	0.986	0.837	0.784
12	1.007	1.03	0.765	0.784
13	0.86	0.871	0.774	0.784
14	1.131	1.198	0.900	0.953
15	1.169	1.226	0.929	0.975

^aThese cases involved a very low aspect ratio fin where the estimated boundary-layer thickness was 55% of the fin height.

Application to the Copperhead Projectile

The configuration consisting of body and tail fin was considered. The Copperhead tail-fin gap is 0.02 in. (5 mm), as can be found in Ref. 2. The g/D ratio is 0.033. However, the existence of the slot ahead of the tail fin, as can be seen in Fig. 1, and the slot flow into the body as given in Ref. 2 might cause the "effective" gap height to be quite different from the physical one. Therefore, the application of the present gap model was considered to provide only an estimate rather than an actual value. One might either increase or decrease the g height to account for this difference; but this variation would be highly arbitrary and cannot be used formally without good justification. Therefore, in the present application, only the physical and true value of 0.02 in. (5 mm) was used. Of course, the larger the effective gap, the larger the normal force loss would be. One other peculiarity to be considered in the case of the Copperhead is the gap blockage or "fin stem interference." As can be found in Ref. 2, the tail-fin stem is quite bulky and is twice the width of the maximum fin-root thickness. This added blockage is certain to reduce the estimated gap losses. All of the data used to formulate the present correlation include a small fin-stem-interference effect, but not for such an unusual blockage. Therefore, it is expected that the present model will predict larger gap losses than those actually incurred for the case of the Copperhead projectile.

The normal-force-slope coefficient with gap effects is given in Fig. 11. The Missile DATCOM code was used to provide the no-gap case, and the modification for the gaps was made using Eqs. (4) and (9) over the extended Mach range of $0.8 \leq M \leq 1.6$.

Slot Effects: Application to the Copperhead Projectile

The same configuration of body and tail fins was considered. The slot effects were modeled using Washington's approach.¹⁴ The corrected normal-force-slope coefficient is given in Fig. 12. As mentioned earlier, that approach is Mach number independent; therefore, the application here was made over the Mach range $0.5 \leq M \leq 1.8$. As in the previous predictions, the DATCOM code results were modified accordingly to provide the new results.

Combined Gap and Slot Effects

The normal force losses due to gaps and slots were combined, and the computed normal-force-slope coefficient is given in Fig. 13 over the extended range $0.8 \leq M \leq 1.6$. The reduction of $C_{N\alpha}$ was about 21% near Mach 1.05.

In the free-flight tests, the projectile is spinning at a moderate rate where the slot and gap effects may differ significantly from those observed in the nonspinning wind-tunnel tests. This explanation may be useful to interpret the large differences noticed between wind-tunnel and firing test data.

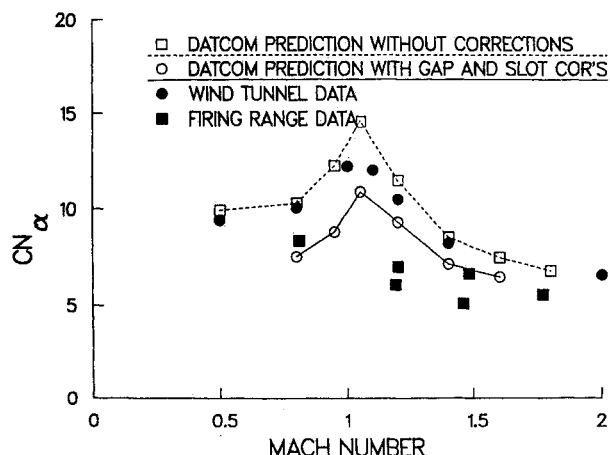


Fig. 13 Gap and slot modeling effects on the normal-force-slope coefficient for the Copperhead projectile.

IV. Conclusions

All known data covering fin-body gap and body slot effects have been surveyed, analyzed, and used. A correlation relation has been established to provide the magnitude of the normal force losses of fins owing to streamwise fin-body gap for any fin shape and gap size in the transonic speed regime of $0.8 \leq M \leq 1.2$ and for $g/D \leq 0.08$. Existing data also support the validity of the correlation in the wider range of $0.7 \leq M \leq 1.3$ without noticeable loss in accuracy. The established correlation is based on all of the experimental data surveyed and has been validated for more than 15 different cases with an accuracy of $\pm 5\%$. This correlation takes into account the variations in fin shape, fin area, fin span, and chord length, gap height, body diameter, and Reynolds number. The correlation is highly useful for including viscous and fin support effects, which are included in the correlation. This approach has advantages over existing inviscid analyses, which cannot be used for small gaps where viscous effects dominate or where the fin support interference is large. The correlation is in algebraic form and uses direct, measurable fin geometry and flight condition inputs. It is simple and can be used in conjunction with any of the fast aerodynamic prediction codes for practical fin design purposes.

Body slot effects on reducing the fin normal force losses were modeled using a previously suggested model.¹⁴ That model was validated in the subsonic speed regime only, although the theory behind it allows it to be used also in supersonic speeds for slender bodies. This model, however, does not account for the slot shape, area, depth, or location relative to the fin. The model is simple and can be directly used in the fast design codes as well. Both models are valid for small angles of attack, usually considered to be in the range $\alpha < \pm 6$ deg.

An application was made to the geometry of the Copperhead guided projectile. That configuration, with very large fin stem and deep slot flow, is not a typical configuration for application of both models. However, the results obtained using those models have shown a reduction of the total normal force and pitching moment by values as large as 21 and 38%,² respectively. Comparison with wind-tunnel and range results showed improved agreement.

Although all of the data used in the present analysis were based on a body with four cruciform fins, the analysis can be used for any set of fins with arbitrary number of panels (≤ 8) at small angles of attack.

Future improvements should consider representing an equivalent streamwise gap height (or gap area) to account for non-streamwise gaps that occur when the control surface is deflected at an angle relative to the body axis. This effect is very important for all guided missiles and projectiles with controllable lifting surfaces.

References

- Mikhail, A. G., "Application and Assessment of Two Fast Codes for a Class of Guided Projectiles," *Journal of Spacecraft and Rockets*, Vol. 4, July-Aug. 1987, pp. 303-310; also U.S. Army Ballistic Research Lab., Aberdeen Proving Ground, MD, BRL-TR-2747, July 1986.
- Mikhail, A. G., "Fin Gaps and Body Slots: Effects and Modeling for Guided Projectiles," AIAA Paper 87-0447, Jan. 1987; also U.S. Army Ballistic Research Lab., Aberdeen Proving Ground, MD, BRL-TR-2808, June 1987.
- Bleviss K. C. and Struble, R. A., "Some Effects of Streamwise Gaps on the Aerodynamic Characteristics of Low Aspect Ratio Lifting Surface at Supersonic Speeds," Douglas Aircraft Co. Rept. SM-14627, April 1953; also U.S. Army Ballistic Research Lab., Aberdeen Proving Ground, MD, BRL-TR-2808, June 1987.
- Mirles, H., "Gap Effect on Slender Wing-Body Interference," *Journal of the Aeronautical Sciences*, Vol. 20, Aug. 1953, pp. 574-575.
- Dugan, W. D. and Hikido, K., "Theoretical Investigation of the Effects Upon Lift of a Gap Between Wing and Body of a Slender Wing-Body Combination," NACA TN-3224, Aug. 1954.
- Hoerner, S. F., *Fluid Dynamic Lift*, published by the author, Chap. 20, p. 17. 1975.

⁷Killough, T. L., "Investigation of Fin Gap Effects on Static Stability Characteristics of Fin Stabilized Missile," U.S. Army Missile Command Rept. RF-TR-64-6, April 1964.

⁸Dahlke, C. W. and Pettis, W., "Normal Force Effectiveness of Several Fin Planforms with Streamwise Gaps at Mach Numbers of 0.8 to 5.0," U.S. Army Missile Command Rept. RD-TR-70-8, April 1970.

⁹Henderson, J. H., "An Investigation of Streamwise Body-Fin Gaps as a Means of Alleviating the Adverse Plume Effects on Missile Longitudinal Stability," U.S. Army Missile Command Rept. RD-77-13, Jan. 1977.

¹⁰Fellows, K. A., "The Effects of Gap Size on the Lift and Drag of a Simple Body with Small Rectangular Wing at Subsonic Speeds," Aircraft Research Assoc., Lt, Test Code M49/15, Bedford, England, June 1982.

¹¹August, H., "Improved Control Surface Effectiveness for Missiles," AIAA Paper 82-0318, Jan. 1982.

¹²Sun, J., Hansen, S. G., Cummings, R. M., and August, H., "Missile Aerodynamic Prediction (MAP) Code," AIAA Paper 84-0389, Jan. 1984.

¹³Appich, W. H. Jr. and Wittmeyer, R. E., "Aerodynamic Effects of Body Slots on a Guided Projectile," *Journal of Spacecraft and Rockets*, Vol. 17, Nov.-Dec. 1980, pp. 522-528.

¹⁴Washington, W. D., Wittmeyer, R. E., and Appich, W. H. Jr., "Body Slot Effects on Wing-Body and Wing-Tail Interference of a Typical Cannon-Launched Guided Projectile," AIAA Paper 80-0260, Jan. 1980.

¹⁵Washington, W. D., Wittmeyer, R. E., and Appich, W. H. Jr., "Design Approach for Estimating Body Slot Effects on Wing-Body-Tail Lift," *Journal of Spacecraft and Rockets*, Vol. 18, Nov.-Dec. 1981, pp. 481-482.

¹⁶Appich, W. H. Jr., McCoy, R. L., and Washington, W. D., "Wind Tunnel and Flight Test Drag Comparison for a Guided Projectile with Cruciform Tails," AIAA Paper 80-0426, Jan. 1980.

¹⁷Pettis, W. C., Nielsen, J. N., and Kattari, G. E., "Lift and Center of Pressure of Wing-Body-Tail Combinations at Subsonic, Transonic and Supersonic Speeds," NACA Rept. 1307, 1959.

¹⁸Schlichting, H., *Boundary-Layer Theory*, 6th ed., McGraw-Hill, New York, 1968, p. 599.

Recommended Reading from the AIAA Progress in Astronautics and Aeronautics Series . . .



Spacecraft Dielectric Material Properties and Spacecraft Charging

Arthur R. Frederickson, David B. Cotts, James A. Wall and Frank L. Bouquet, editors

This book treats a confluence of the disciplines of spacecraft charging, polymer chemistry, and radiation effects to help satellite designers choose dielectrics, especially polymers, that avoid charging problems. It proposes promising conductive polymer candidates, and indicates by example and by reference to the literature how the conductivity and radiation hardness of dielectrics in general can be tested. The field of semi-insulating polymers is beginning to blossom and provides most of the current information. The book surveys a great deal of literature on existing and potential polymers proposed for noncharging spacecraft applications. Some of the difficulties of accelerated testing are discussed, and suggestions for their resolution are made. The discussion includes extensive reference to the literature on conductivity measurements.

TO ORDER: Write AIAA Order Department,
370 L'Enfant Promenade, S.W., Washington, DC 20024
Please include postage and handling fee of \$4.50 with all
orders. California and D.C. residents must add 6% sales
tax. All orders under \$50.00 must be prepaid. All foreign
orders must be prepaid.

1986 96 pp., illus. Hardback
ISBN 0-930403-17-7
AIAA Members \$26.95
Nonmembers \$34.95
Order Number V-107